Detailed Modeling of Integrated IQ-Transmitters for 100G+ Applications

A. Richter*[a], C. Arellano[a], D. Carrara[c], S. Mingaleev[b], E. Sokolov[b], I. Koltchanov[a]

[a]VPIsystems, Carnotstr. 6, 10587 Berlin, Germany;
[b]VPI Development Center, Chapaeva str. 5, 220034 Minsk, Belarus;
[c]CNRS, Telecom SudParis, 9 rue Charles Fourier 91011 Evry, France

ABSTRACT

We present techniques for modeling the physics and systems-level characteristics of integrated IQ-transmitters for 100G+ applications and emphasize important design aspects. Using time-and-frequency-domain modeling (TFDM) of Photonic Integrated Circuits (PIC), we present a detailed IQ-transmitter model based on the physics and setup of active and passive subcomponents. With this, we link characteristics of subcomponents (bending loss of waveguides, phase changes in MMI couplers, sweep-out time of EAMs) to systems-level characteristics of the integrated IQ-transmitter (extinction ratio, modulation bandwidth, chirp). Further, a behavioral transmitter model is introduced and utilized to assess electrical driving requirements (allowed jitter, noise, synchronization offset).

Keywords: photonic integrated circuit, photonic simulator, design, modeling

1. INTRODUCTION

Photonic Design Automation (PDA) plays a significant role when designing sophisticated photonic circuits performing very complex functions by providing a compliant, time-efficient and reliable simulation environment. One of the key technologies of modern 100G applications is the in-phase/quadrature (IQ) transmitter representing a versatile optical transmitter concept supporting various multilevel modulation formats as it allows direct electronic encoding of arbitrary points on the complex signal constellation plane. Further on, the optical transmission channel becomes transparent to the applied electrical drive signal in conjunction with coherent optical detection, allowing the application of powerful electronic signal processing techniques.

Using time-and-frequency-domain modeling (TFDM) of a Photonic Integrated Circuit (PIC) [1], we derive detailed IQ-transmitter models based on the physics and architecture of the underlying active and passive subcomponents. This modeling approach allows linking characteristics of subcomponents (such as bending loss of waveguides, phase changes in multimode interference couplers, sweep-out time of electro-absorption sections) to systems-level characteristics of the integrated IQ-transmitter (such as extinction ratio, modulation bandwidth, chirp). On the systems design side, a behavioral transmitter model based on measured and simpler parametric characteristics is more appropriate, though. Such a model can be used for instance to derive electrical driving requirements (allowed jitter, noise, synchronization offset) and assess for various modulation formats the impact of transmitter limitations (modulation bandwidth, chirp) on system performance.

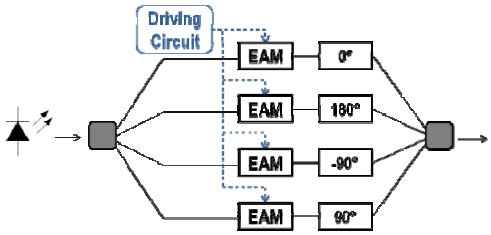

Figure 1. Block diagram of the vector-transmitter

*andre.richter@vpiphotonics.com; phone +49 30 398058 0; fax +49 30 398058 58; www.VPIphotonics.com

Next-Generation Optical Communication: Components, Sub-Systems, and Systems,
edited by Guifang Li, Dieter Stefan Jäger, Proc. of SPIE Vol. 8284, 82840L · © 2012 SPIE
CCC code: 0277-786X/12/$18 · doi: 10.1117/12.912096

We present with this contribution different techniques for modeling the physics and systems-level characteristics of integrated IQ-transmitters for 100G applications with typical multilevel modulation formats. Further we point to important design aspects by means of several application examples. The following analysis is based on a new vector electroabsorption-based modulator (EAM) transmitter (Figure 1), which is being developed in frame of the European research project MIRTHE [2].

2. BEHAVIORAL MODEL APPROACH

Starting from the physical design of the transmitter, a behavioral model based on measured and parametric characteristics is derived, which is appropriate for the analysis and performance evaluation of the PIC when operated in various transmission systems and applying different modulation approaches.

Its schematic is represented in Figure 2. The optical output of a CW-laser source is fed into an ideal splitter which divides the optical power into four branches. Each branch contains an EAM and a phase shifter. The four EAMs are modulated with electrical voltages containing in-phase (I) and quadrature (Q) data signal information. The modulated signals are combined in an ideal coupler. This behavioral design can represent both, the ideal model and a more realistic one that accounts for non-linear transmission and alpha factor characteristics of the EAMs, and non-ideal driving circuits. This type of model assists for instance by optimizing the driving conditions of the EAMs: depending on the specific EAM characteristics driving parameters can be adjusted such that the EAMs are operated in its linear region.

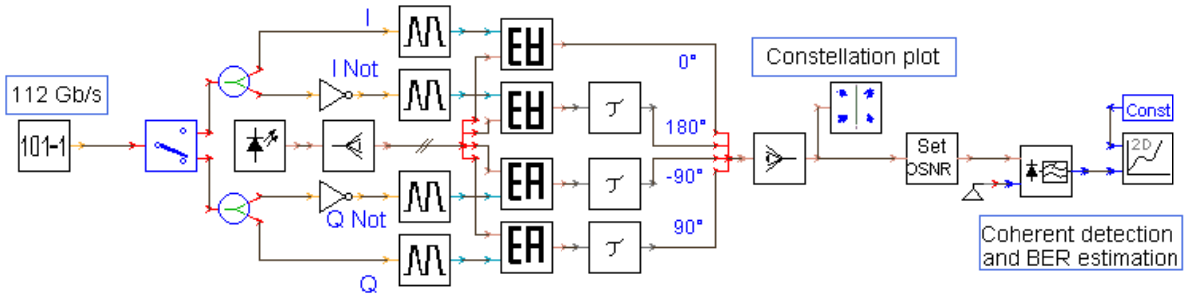

Figure 2. Schematic of the simulated transmission system, comprising the behavioral model of the transmitter, plus optical noise and coherent detection using VPItransmissionMaker Optical Systems v8.6

2.1 EAM - non-linear voltage-dependencies

Voltage-dependent transmission and chirp characteristics of EAMs can be described by analytic functions generated on the basis of hyperbolic expressions and experimental measurements (Figure 3).

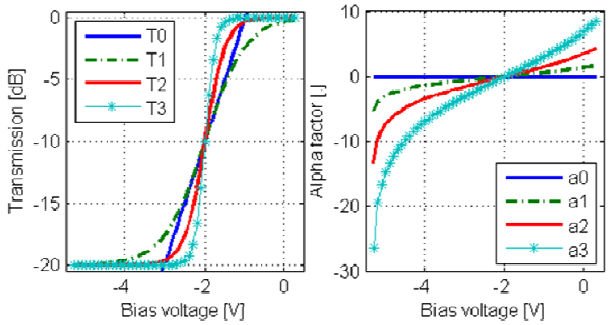

Figure 3. Overview of simulated transmission (left) and chirp (right) characteristics of the EAMs

A non-linear transmission characteristic is not a major drawback, provided that the EAMs are biased at a linear segment, around the working point. The chirp causes a rotation in the constellation diagram and symbol-dependent

transitions that together with differences in the electrical path would cause an unequal rotation of the points in the constellation diagram, which is difficult to recover by means of phase correction mechanisms at the receiver, especially in denser constellation, such as 16QAM signal (Figure 4). These effects limit the achievable modulation rate.

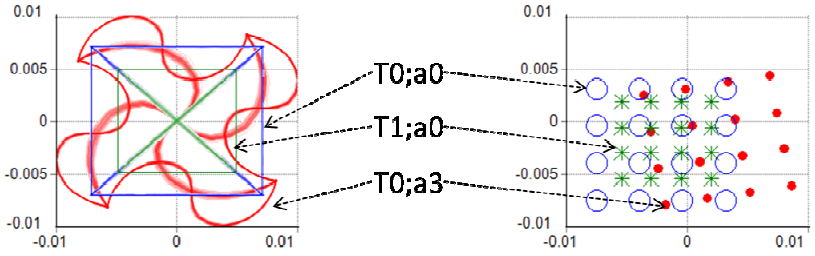

Figure 4. Constellation diagrams for QPSK and 16QAM for different characteristics of the EAMs: (T0;a0), (T1;a0) and (T0;a3), as shown in Figure 3. Note: the asymmetric constellation for 16QAM has been obtained using the QPSK transmitter with additional attenuators in the inner branches.

2.2 Jitter and synchronization offset

Operating the EAMs in their respective saturation regions causes a compression of the constellation diagram, which may result in reduced signal quality. For modulation formats with multiple amplitude levels (such as square 16QAM constellation), for instance, the outermost constellation points move closer to the inner ones increasing the impact of additive noise on signal performance. Further on, the detrimental influence of the modulator chirp might prohibit large driving amplitudes (Figure 5, left).

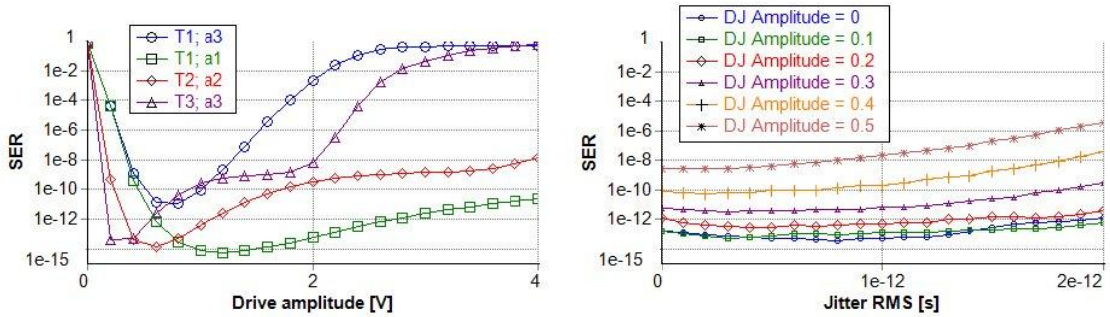

Figure 5. 112Gb/s QPSK with OSNR=25dB; left: symbol error rate (SER) versus drive amplitude for different EAM characteristics (from Figure 3); right: SER as function of deterministic jitter (DJ) and Gaussian random jitter of the electrical circuits.

The impact of asynchronization of the four electrical paths can be tested by adding a deterministic jitter to the driving signals. Results for a sinusoidal jitter (10GHz) reveal a high response to synchronization offsets. On the other hand, such a transmitter is relatively robust to random jitter variations. This is also due to the nature of the coherent detection configuration (Figure 5, right).

3. DETAILED PHOTONIC INTEGRATED CIRCUIT APPROACH

Within our circuit-level modeling approach, complex transmitter and receiver structures are considered as photonic integrated circuits that are composed of several active and/or passive sub-elements. It is based on segmentation of the modeled PIC into smaller building blocks (PIC elements). Each PIC element is a photonic device that is coupled to other PIC elements via guided modes of channel optical waveguides, called ports. In that way, each PIC element is considered as black-box that produces outgoing waves carried by guided modes of the device ports from the corresponding incoming waves (Figure 6).

This approach allows separating circuit-level modeling of PICs from device-level modeling of PIC elements, so that different PIC elements in the same circuit can be modeled by different methods and simulation accuracy. Passive elements are described in terms of frequency defined S-matrices, while active parts are modeled in the time domain by means of the transmission-line model (TLM). Passive PICs, consisting of linear PIC elements only, can be efficiently modeled in the frequency domain. However, the presence of non-passive PIC elements, such as lasers, SOAs, and modulators requires of a time-domain simulation solution. In that case, we recently introduced the new hybrid Time-and-Frequency-Domain Modeling (TFDM) solution [1].

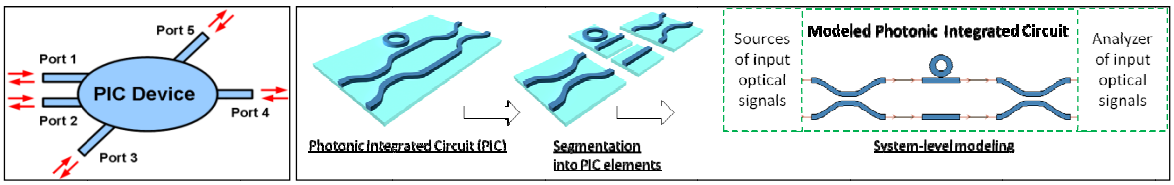

Figure 6. Representation of a 5-port PIC device (left) and PIC simulation based on segmentation into fundamental sub-elements (right)

The detailed PIC model of the concerned IQ transmitter is represented in Figure 7. It comprises TLM-based models for active elements (DFB laser and EAMs), MMI modules intended for splitting and coupling, bent-waveguides and scattering elements that represent S-bends in the PIC circuit, and straight optical waveguides that carry out optical phase shifting. More details of the models can be found in [3-4]. We analyze two different designs of coupling the signals at the output, one using a single 4x1-MMI coupler and one using two stages of 2x1-MMI couplers.

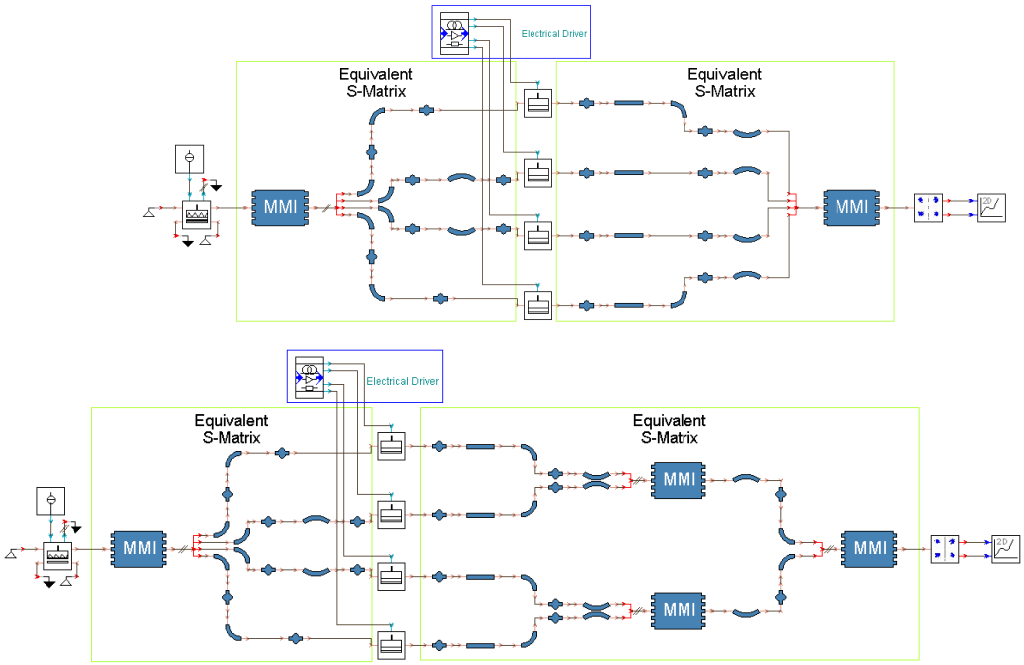

Figure 7. Schematics of the simulated transmitter for two types of output couplings: using a single 4x1-MMI coupler (top) and using two stages of 2x1-MMI couplers (bottom) in VPIcomponentMaker Photonic Circuits v8.6.

In a hybrid structure such as investigated here, TFDM greatly improves the simulation speed and required memory for the same numerical accuracy. Clusters of interconnected passive PIC elements are represented by their equivalent S-matrices, which are constructed from the combination of the individual S-matrices of each PIC element. Then, FIR filters are designed for each equivalent S-matrix and a time-domain simulation is executed for modeling the properties of the integrated PIC.

The simulation speed improvement depends on multiple factors, foremost on the complexity of the design (e.g., many passive sub-elements, possibly with feedback loops). The overall speed and accuracy is determined by the number of simulated time samples and used time step. Note that the minimum number of processed samples depends on the required time and frequency resolution of the PIC which ensures the desired accuracy value (e.g., the shortest sub-element, or the active section with the fastest/widest gain dynamics), and on the modeling task itself (e.g., display of constellation diagram, or calculation of SER). In this example, the simulation speed improves by 50% when compared to a pure time-domain simulations when using a moderate number of samples.

4. DESIGN ASPECTS OF PIC SUB-COMPONENTS

4.1 Reflections at facets of active elements: laser, EAM and SOA

Unwanted feedback into the active region of the active subparts, laser, absorber or SOA might cause disturbing fluctuations of the optical power and phase resulting into patterning effects at the output of the device. For studying such effects, we reduce the transmitter structure to a model comprising laser, EAM, and SOA with attenuators in between representing the loss of passive elements in between (Figure 8). This model can account for variable reflectivity and phase change at each of the facets. In this setup, the facet reflectivity right of the DFB laser and EAM represent potential reflections at the active-passive material interface. The facet reflectivity right of SOA represents potential reflections at the output interface of the transmitter.

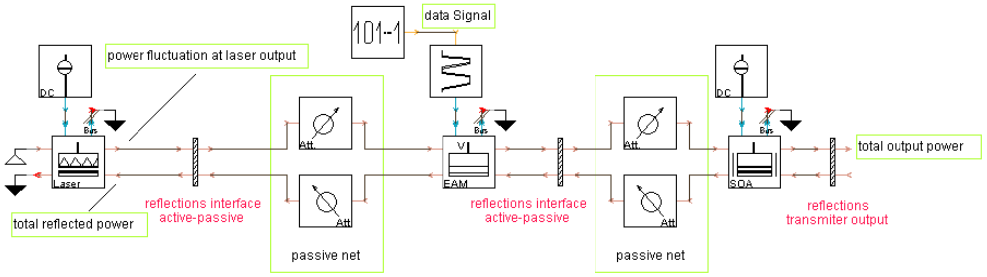

Figure 8. Setup of the simplified transmitter for studying the impact of reflections

The laser is biased with 100mA to generate 12dBm optical power at its output. For simplification, the passive net is considered to be symmetric in terms of attenuation: we applied 5dB attenuation in forward and backward direction representing splitting, coupling and waveguide loss. The EAM is reverse biased between -5V and 0V, and modulated with a 40Gb/s data signal (note that this is rather optimistic considering the aim to study only the effect of reflections). The bias current applied to the SOA has been varied and increased up to 200mA, what results in an optical power of up to -1dBm at the transmitter output. We applied different tests with varied reflection values at different points along the transmitter demonstrating the impact of reflection on the transmitter operation (Figure 9).

The impact of reflections at the active-passive interface remains constant for different levels of amplification and is slightly lower than the one caused by reflections at the end of the device. Reflections at the end of the device are enhanced due to re-amplification and might be critical for high levels of output power. For the presented case, transmitter operation becomes critical for required output powers of 0dBm and more, if the reflection backwards into the laser should be less than 30dB (in order to not disturb the laser operation). Consequently, it is generally of high interest to increase the output power of the laser and work on decreasing the loss of passive waveguides and other connecting elements before considering solutions that integrate an additional amplification section into the transmitter design.

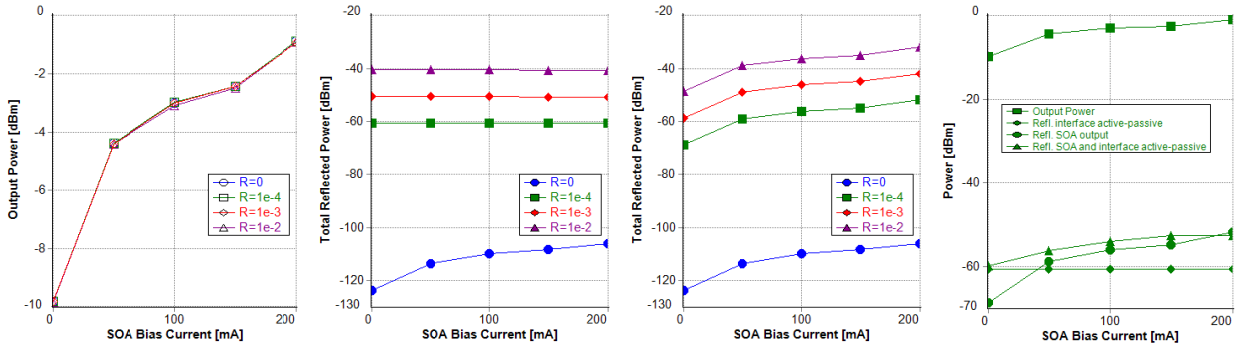

Figure 9. (From left to right): Power at transmitter output for different values of reflection and SOA bias current. Total reflected power traveling backwards collected at the laser for reflections at the active-passive interfaces only. Total reflected power backwards collected at the laser for reflections at the transmitter output interface only. Output and reflected powers for R=1e-4 at different parts in the device.

Even though the total output power remains quite constant in average for the different cases we studied, strong power fluctuations at the laser output occur. The impact on the signal quality can be clearly seen when analyzing the eye diagram (Figure 10): pattern effects increase for higher values of reflection.

Other aspects that are also of importance in MQW structures are the carrier sweep-out time of absorbers and the capture and escape time in gain mediums. Time constants contribute significantly to an effective gain compression, and thus, to the limited modulation bandwidth of MQW-based devices. This phenomenon is also investigated in this setup for a 40Gb/s NRZ data signal. As expected, the obtained eye diagrams (Figure 11) reveal that a long capture time (mainly due to carrier diffusion) causes gain compression and thus reduction of extinction ratio, while a longer sweep-out time improves the absorption characteristic and thus increases the signal extinction ratio.

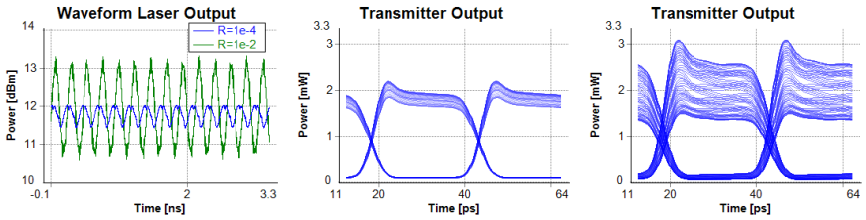

Figure 10. Left: power fluctuations in time at the laser output for R=1e-4 and R=1e-2. Eye diagrams of an alternating data signal at 40Gb/s for R=1e-4 (center) and R=1e-2 (right).

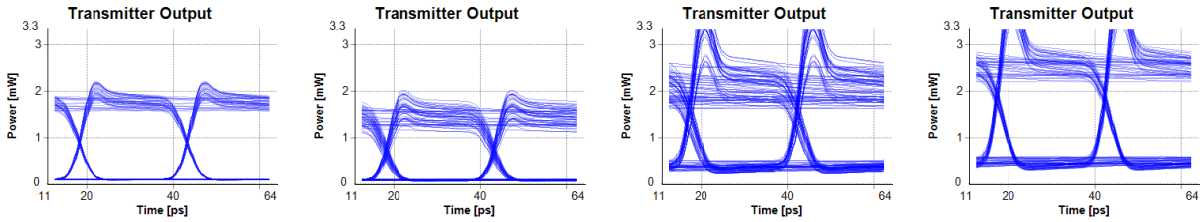

Ts= 8ps, Tc=70ps *Ts= 8ps, Tc=700ps* *Ts= 25ps, Tc=700ps* *Ts= 25ps, Tc=70ps*

Figure 11. Eye diagrams of modulated 40Gb/s NRZ signal for R=1e-4 and different values of sweep-out time (Ts) and capture time (Tc).

4.2 Tolerance of MMI dimensions and phase shifters

Tolerances of the fabrication process as well as accuracy in the phase shifters or additional phase variations introduced at the passive waveguides, might lead to non-optimal splitting operations. This problem is analyzed for the two setups represented in Figure 7. We use a 112Gb/s QPSK-modulated signal with 25dB OSNR and a coherent receiver including SER estimation.

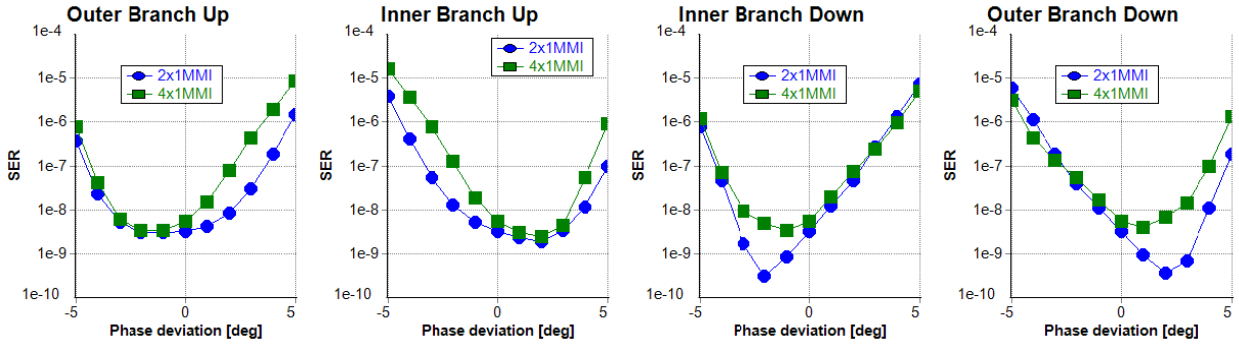

Figure 12. SER as function of phase deviations in the phase shifters at the different branches in the transmitter

At first we introduce a phase deviation at the different branches in the device. The results for the different cases (Figure 12) reveal the tendency that both structures behave similarly: there is an optimum phase shift that is slightly different then the theoretical one (Figure 1). This effect occurs because signals at each branch are not in phase, as a result of the different phases at the output of the 1x4-MMI splitter and the additional chirp introduced by the EAMs. From the obtained curves we gather that the configuration with a single 4x1-MMI coupler is more sensitive to such imperfections. Further we note that the signal in-phase tributary (inner and outer branches up) is more affected by phase imperfections, probably because of the combination of phase deviations accumulated along the PIC in this design.

Within the scope of a second analysis, variations with respect to the designed dimensions of the different MMIs are introduced in the model, at the 1x4-MMI splitter, and at the different MMI-couplers at the output of the transmitter. Simulation results (Figure 13) demonstrate that small width variations introduce already detectable signal performance degradations. Imperfections in the first and last MMI elements are not critical for small deviations. However, for the transmitter with two-stage 2x1-MMI couplers, the margin of tolerance is tighter.

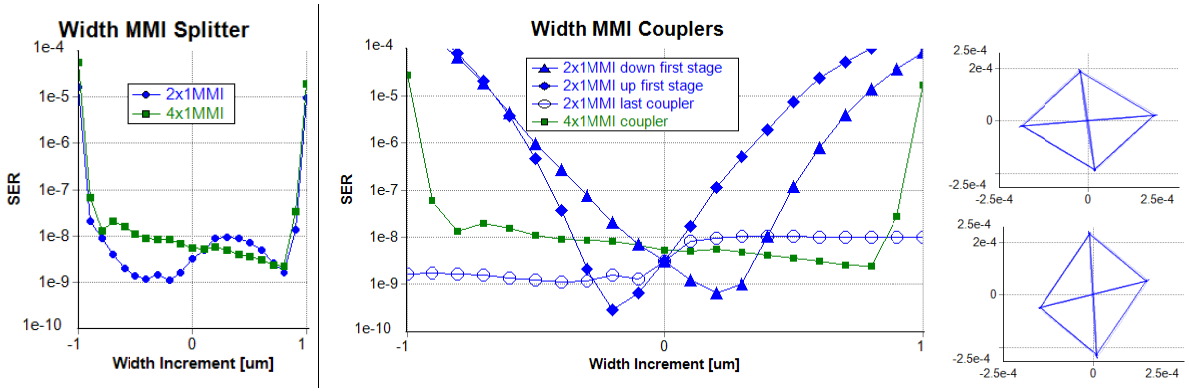

Figure 13. SER as function of width variations in MMI devices: at the 1x4-MMI splitter (left), at the different MMI couplers (center); constellation diagrams for 0.5um width increment in the 4x1-MMI coupler (right-top) and in the upper 2x1-MMI coupler in the two stage design (right-bottom).

SUMMARY

Several techniques for modeling different design characteristics of integrated IQ-transmitters have been described by means of modeling with different level of abstraction. A behavioral modeling approach has been used to determine the effect of chirp introduced by EAMs and to analyze the electronic circuit in terms of applied voltage, jitter and synchronization. Non-ideal characteristics of the EAM introduce rotation and contraction of the constellation diagram, which is more severe in the case of non-linear dependencies. These degradations affect the extinction ratio of the signal and also the achievable modulation rate. Random jitter of the electrical drive is not a problem in such transmitters, if kept within an acceptable range. However, the design is rather sensitive to asynchronization of the electrical paths. A detailed circuit model of the transmitter, considering it as a photonic integrated circuit has been introduced for a more comprehensive analysis based on physical characteristics of the PIC sub-elements. Reflections at the interface of active-passive elements are more significant as when they occur at the end of the device. Phase changes and alterations in the dimensions of MMI coupling elements also constraint the modulation performance, even producing non-linear effects.

ACKNOWLEDGMENTS

This work has been partially funded by the EU FP7/2007-2013 under the grant agreement n° 257980 (MIRTHE). The authors thank Christophe Kazmierski and David Carrara from III-V Labs for valuable comments.

REFERENCES

[1] Mingaleev, S.F., Sokolov, E., Arellano, C., Koltchanov, I., Richter, A., "Hybrid Time-plus-Frequency-Domain Approach to Modeling Photonic Integrated Circuits," NUSOD, paper ThA4 (2011).
[2] http://www.ist-mirthe.eu/
[3] Arellano, C., Mingaleev, S.F., Novitsky, A., Koltchanov, I., Richter, A., "Design of Complex Semiconductor Integrated Structures," ACP, paper WD4 (2009).
[4] Arellano, C., Mingaleev, S.F., Sokolov, E., Koltchanov, I., Richter, A., "Efficient Design of Photonic Integrated Circuits (PICs)," ICTON, paper Th.A4.1 (2011).